Fluid geochemistry and geothermal prospectivity of the Taranaki and Hikurangi Forearc hydrocarbon-bearing sedimentary basins, New Zealand

A.G. Reyes

GNS-Science 1 Fairway Drive Avalon, Lower Hutt, New Zealand

a.reyes@gns.cri.nz

Keywords: sedimentary basins, petroleum, geochemistry, Taranaki, Hikurangi, New Zealand

ABSTRACT

The geothermal prospectivity of Taranaki is deemed 6th and the Subaerial Hikurangi Forearc (SHF) 7th, of the 17 low-enthalpy geothermal regions in New Zealand. The minimum recoverable heat in Taranaki is ~0.54 PJ/a with estimated temperatures at depth as high as 200ºC. In contrast the minimum recoverable heat in the SHF is ~0.29 PJ/a with thermal reservoir temperatures as high as 140ºC. Thermal reservoirs >100ºC can be intersected by wells drilled ≥3.0 km in Taranaki and mostly ≥3.5 km in the SHF. More than 85 petroleum wells in Taranaki have already intersected >100ºC thermal reservoirs compared to <5 in the SHF . Because of the likelihood of liquid condensation, the presence of >C6 hydrocarbon gases would require a different distribution system for geothermal fluids for power or direct heat use if fluids from petroleum wells are directly harnessed for geothermal energy. However, the use of deep borehole heat exchangers may obviate the problem of hydrocarbon gas condensation and hydrocarbon solidification during geothermal production.

1. INTRODUCTION

1.1 Study Areas

There are 17 low-temperature regions in New Zealand, outside the high-temperature volcanic geothermal systems in the Taupo Volcanic Zone and Ngawha (Reyes et al, 2010), with most having estimated subsurface temperatures of 100-200ºC and a high of 250ºC in the Coromandel Peninsula (Fig. 1). The focus of this study are two sedimentary basins: Taranaki in the west and the Subaerial Hikurangi Forearc (SHF), the subaerial extension of the East Coast basin. These two areas were selected because of differences in tectonic setting and heat flow regimes and also because the largest number of abandoned/unused petroleum wells were drilled in these areas. In this paper, "unused" refers to wells that are plugged, abandoned and plugged, suspended or of unknown status. There are ~700 unused petroleum wells in onshore New Zealand with 42% located in Taranaki, 13% in the SHF and the rest distributed in various low-temperature regions of the South Island and other areas of the North Island (Fig. 1).

Part of this study is focused on unused petroleum wells for future geothermal retrofitting spurred on by (1) the government's initiative, under the Paris Agreement, to reduce greenhouse gas emissions by 30% below 2005 levels by 2030 and to attain carbon neutrality by 2050 (www.mfe.govt.nz) and (2) the decline and nearing end of life of hydrocarbon reserves in Taranaki (Reyes, 2019). Using abandoned petroleum wells will cut geothermal development costs not only because of the ready-made infrastructures but also because of (1) the large amount of publicly-available data such as seismic surveys of the regions and subsurface data from well drilling e.g., geology including lithology, stratigraphy and structures; formation properties such as porosity and permeability; reservoir pressures; fluid salinity and gas compositions; gas and water flow rates; well temperatures during drilling and estimated bottomhole temperatures (BHT); drilling history including mud losses and the state of the well (www.nzpam.govt.nz) and (2) availability of cuttings and sidewall cores from wells. Although several countries have harnessed geothermal power from low-temperature sedimentary systems and also abandoned petroleum wells (e.g., Wang et al, 2016; Wanner et al, 2017; Liu et al, 2018; https://www.powerelectronicsnews.com), the long-term success of this source of geothermal energy in New Zealand is still unknown. Furthermore, conversion of a petroleum system to a geothermal-producing region has to overcome various still-unstudied factors in New Zealand including well ownership and socio-economic, environmental, scientific and technical hurdles (e.g., Reyes, 2007; 2015; 2019).

The objective of this study is to compare the sources of heat and fluids, temperatures at depth and general geothermal characteristics of Taranaki and the SHF based on chemical compositions of well discharges and natural surface manifestations, and well bottomhole temperatures (BHT).

2. GEOLOGY

The Taranaki Peninsula is within a 100,000 km^2 sedimentary basin that extends mostly offshore (Palmer and Andrews, 1993; King and Thrasher, 1996), with a basin fill of up to 9000 m of Cretaceous to Quaternary rocks (www.mbie.govt.nz; Townsend et al, 2008). The peninsula covers about 3500 km^2 west of the Taranaki Fault (Fig. 2A), comprising ~3.5% of the Taranaki Basin. Andesitic volcanoes at Taranaki are the most westerly expression of subduction related andesitic volcanism in New Zealand (Locke et al, 1994) where the subduction interface is estimated to be at ~ -250 km depth (Williams et al, 2013). The volcanoes become younger from 1.8 Ma at Motumahanga/Sugar Loaf Islands and Paritutu in the north to Egmont (<130 ka) and Fantham's Peak (<3.2ka) in the south (Townsend et al, 2008). Taranaki is the only oil, gas and condensate producing basin in the country (www.mbie.govt.nz) where the onshore region has ~300 plugged and abandoned/unused wells (Fig. 2A) and >150 actively used for oil and gas/condensate production and injection (https://data.nzpam.govt.nz). There are ~100 cold springs and gas vents of which ~20% are petroliferous. No hot springs have been located in the peninsula since the early 2000's (Reyes field notes). Oil seeps and gas vents at New Plymouth spurred drilling for oil in the area as early as 1866 (de Coury Clarke, 1912). But with the discovery of gas at Kapuni in 1959, the focus of

hydrocarbon exploration shifted to Eocene and later Miocene to Pliocene sediments away from New Plymouth (Smale et al, 1999; www.mbie.govt.nz). Active faults generally strike NE-SW (Fig. 2A).

The Subaerial Hikurangi Forearc (SHF) covers 14% of the total 180,000 km^2 of the East Coast basin (https://www.nzpam.govt.nz) and is at the leading edge of subduction along the Hikurangi margin where the subduction depth is at -40 km and shallower (Williams et al, 2013). There are ~500 cold springs and gas vents of which 8% are petroliferous. The two hot springs expel 71^{o}C (Te Puia) and 50^{o}C (Morere) high-Cl aqueous fluids (Fig. 2B). The anomalous presence of hot springs in a region of generally low heat flow (e.g., Allis et al, 1998) is attributed to hotter crust in the north (Field et al, 1997) where the hot springs are located and to rapid ascent of aqueous solutions that originate from greater depths, near the subduction interface (Reyes et al, 2022; Reyes and Hall, 2022). Cold mud volcanoes are common along the length of the SHF (Reyes et al, 2022). About 90 wells have been drilled in the area from 1875 to 2013 (https://data.nzpam.govt.nz) with a few oil producers. However, unlike Taranaki, the SHF is not a commercial petroleum producer at present.

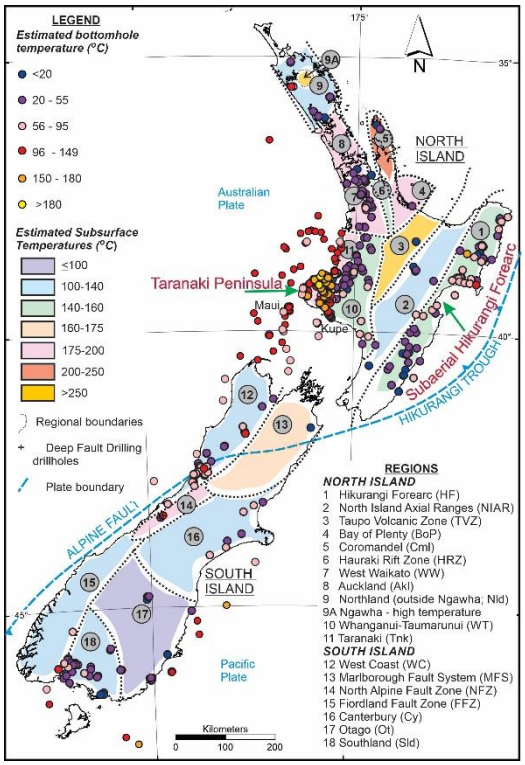

Figure 1: Map of New Zealand showing estimated subsurface temperatures of geothermal regions (adapted from Reyes, 2018), location and bottomhole temperatures of petroleum wells (this study) and the boundary between the Australian and Pacific plates (e.g., Townend et al, 2012). Subduction is initiated along the Hikurangi Trough.

3. UNUSED PETROLEUM WELLS AND BOTTOMHOLE TEMPERATURES

Total vertical depths of abandoned wells range from <20 to 5680 m, with >4000 m deep wells located in Taranaki except for one 4350 m deep well in the SHF (Rere-1). In the absence of stabilized measured downhole well temperatures for most petroleum wells, bottomhole temperatures (BHT) are estimated using published surface conductive heat flow data (Funnell et al, 1996; King and Trasher, 1996; Funnell and Allis, 1997; Field et al, 1997; Allis et al, 1998; Cook et al, 1999) and converted to thermal gradient in ^{o}C/km using a factor of 2.1 (Funnell et al, 1996) and an average ambient air temperature of 15^{o}C. The heat flow values in the Taranaki Peninsula varies from as high as 70-74 mW/m^2 in the north to 50 mW/m^2 in the south (Fig. 2A), with the higher values associated with Quaternary volcanism (Funnell et al, 1996). Heat flow in the SHF is less varied, at 45 mW/m^2 in the south to 60 mW/m^2 in the north (Allis et al, 1998). A localized high of 170 mW/m^2 at Rotokautuku in the north (Fig. 2B) is attributed to fluid advection (Field et al, 1997) most likely associated with rapidly ascending fluids above the subduction interface along cross-cutting EW, NE-SW and NW-SE trending faults (Reyes et al, 2022). Thermal gradients in abandoned wells in Taranaki ranges from 23-35^{o}C/km compared to mostly 21-33^{o}C/km in the SHF except in wells near Rotokautuku where the thermal gradient varies from 42-81^{o}C/km (Fig. 3).

BHT values in Taranaki vary from 15^{o}C to a high of 180^{o}C at 4995 mTVD (Total Vertical Depth) at Kaimiro-1 and 200^{o}C at 5550 mTVD at Waimanu-1 with both wells located within the 70 mW/m^2 isocontour. The highest BHT in the SHF is 140^{o}C at 4350 mTVD in the deepest well, Rere-1, located in the north. Estimated BHT values appear to be minimum temperatures based on comparison with measured downhole temperatures in a few wells (e.g., Field et al, 1997), homogenization temperatures in the latest fluid inclusions in quartz grains (Reyes, 1998; Reyes 2015; Reyes unpublished results) and gas temperatures, discussed in Section 4.2.

Figure 3 summarizes the general usage based on BHT and possible conventional and EGS (Enhanced Geothermal System) geothermal retrofitting development methods for existing unused petroleum wells (e.g., Zhu et al, 2019) based on temperature and total vertical depth (Reyes, 2018). All wells can potentially be harnessed for direct heat utilization, especially in industry-heavy Taranaki. Assuming a cut-off temperature of ~100^{o}C, ~87 wells in Taranaki can be harnessed for power generation compared to only two in

the SHF. Shallow heat (<1000 m) can be harnessed using ground source heat pumps (GSHP), bore hole heat exchangers (BHE) equipped with geothermal heat pumps and for >1000 m, deep bore hole heat exchangers.

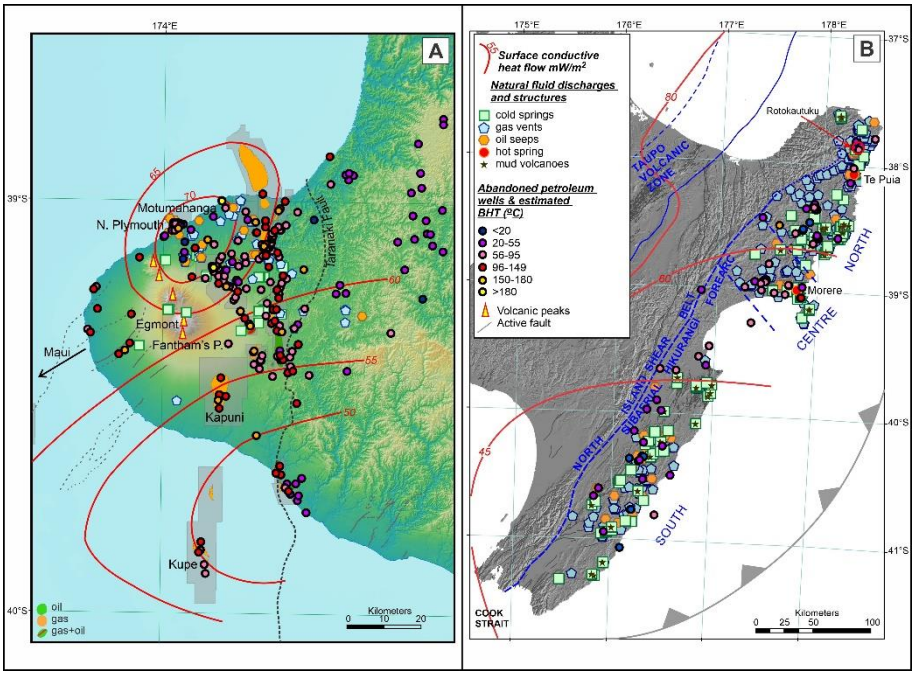

Figure 2: Maps of [A] Taranaki peninsula and [B] the Subaerial Hikurangi Forearc (SHF) showing surface conductive heat flow contours, distribution of natural surface fluid discharges, abandoned petroleum wells and bottomhole temperature (BHT) ranges and main structures (Funnell et al, 1996; King and Trasher, 1997; Allis et al, 1998; Townsend et al, 2008; Reyes et al, 2010 and 2022; this study from various sources; https://data.nzpam.govt.nz).

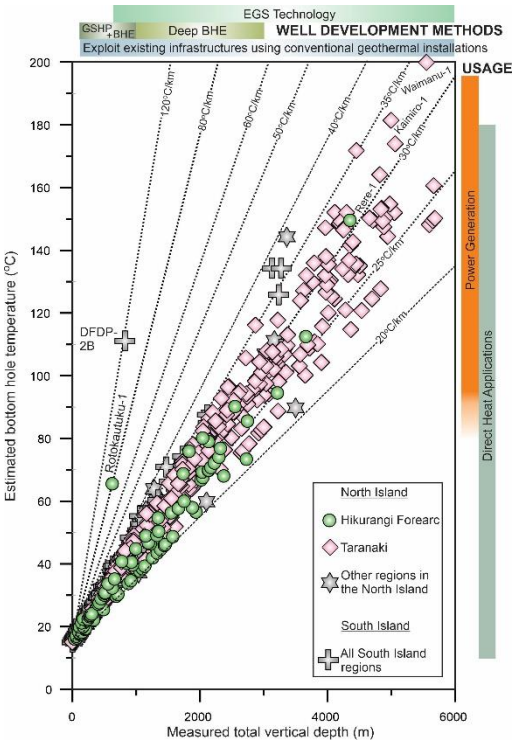

Figure 3: Cross plot of measured total vertical depth vs estimated bottomhole temperature of unused petroleum wells in Taranaki and SHF and other onshore regions in New Zealand, general uses on the right and possible well development methods on top (adapted from Reyes, 2018). Also shown are geothermal gradients in ºC/km.

A previous study (Reyes, 2015) estimated a minimum recoverable heat in Taranaki of ~0.54 PJ/a based on abandoned well discharges compared to ~0.29 PJ/a in the SHF based on spring and well discharges. Of the 17 low-enthalpy geothermal regions in New Zealand, the geothermal prospectivity of Taranaki is ranked 6th and the SHF 7th.

4. FLUID CHEMISTRY

4.1 Aqueous Fluids

4.1.1 Sources

Cold springs in Taranaki have been described as Na-Cl (Henderson and Ongley, 1923), chalybeate forming iron stains, or depositing travertine (de Courcy Clarke, 1912). The few spring samples analyzed are Na-Ca-HCO_3 in composition. Most of the available fluid chemical analyses in Taranaki are well discharges where ~45% of the wells expel Na-Cl, 30% Na-Ca-Cl, 15% Na-HCO_3-Cl and 10% Na-HCO_3 aqueous fluids. Fluid inclusion (Reyes, 1998; Taylor, 2002; Killops et al, 2009; Reyes, unpublished work) and fluid chemistry studies (e.g., Lyon et al, 1996; this study) suggest that aqueous fluid compositions within the Eocene and Miocene sedimentary formations in Taranaki vary in salinity and oil, gas and condensate contents. Aqueous fluids discharged by wells in this study are assumed to be a combination from different sedimentary formations. Based on relative Cl, B and Li compositions (Fig. 4A), Na-Cl aqueous discharges from Ngatoro (Ng) and Kaimiro (Km) wells appear to be a mixture of seawater (sw) and sedimentary formation waters (curve 4) being diluted with meteoric water whilst Na-Cl discharges from "Mckee" (Mc; see Fig. 8 for wells included in this group), Wharehuia (Wh) and Waihapa (W) contain relatively less seawater but more sedimentary formation water mixed with meteoric water (curve 5). There are two Kapuni points. One appears to be a product of mixing of Na-Cl sedimentary formation fluids and meteoric waters (Kapuni-11), resulting to Na-HCO_3-Cl fluids whilst the other consists of hot greywacke water mixing with sedimentary formation water and then diluted by meteoric water (curve 6; Kapuni-15) where the discharge fluid is Na-HCO_3.

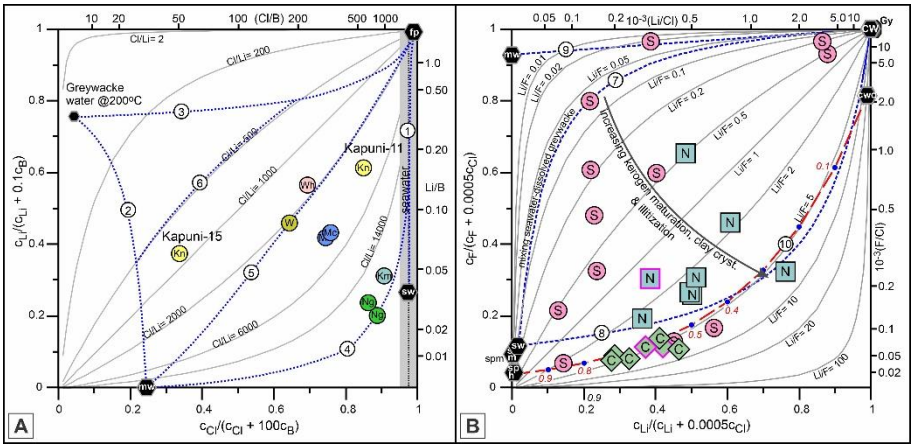

Figure 4: [A] $c_{Cl}/(c_{Cl}+100c_B)$ vs $c_{Li}/(c_{Li}+0.1_B)$ plot of Taranaki and [B] $c_{Li}/(c_{Li}+0.0005c_{Cl})$ vs $c_F/(c_F+0.0005c_{Cl})$ plot of subaerial Hikurangi forearc aqueous fluid discharges. fp= sedimentary formation water; mw= meteoric water; sw= seawater; cw= clay water of dehydration; gy= congruently dissolved greywacke; cwd= mixture of 0.95 greywacke and 0.05 clay water of dehydration (Reyes et al, 2022); sm= Marianas Trench water of serpentinization (Hulme et al, 2010); sph= estimated composition of water of serpentinization in the SHF. Line 1= mixing of sw and fp; curve 2= mixing of meteoric water and greywacke water at 200ºC (Ellis and Mahon, 1967); curve 3= mixing of fp and greywacke water; line 9= mixing of cw and mw. Refer to text for other mixing lines and curves, Fig. 8 for symbols and Figs. 1, 11A and B for map locations of areas.

Most samples evaluated for SHF are from cold springs and two hot springs with a few well discharges. Chloride-rich discharges in the SHF consist of Na-Cl, Na-Ca-Cl or Na-(Ca)-HCO_3-Cl fluids with the last type a mixture of meteoric water and Cl-rich fluids. In the $c_{Li}/(c_{Li}+0.0005c_{Cl})$ vs $c_F/(c_F+0.0005c_{Cl})$ plot (Fig. 4B), Na-Cl aqueous fluids in the SHF lie between curves 7 (greywacke and seawater mixing) and 8 (claywater of dehydration and seawater mixing) with changes from curve 7 to 8 caused by maturation of kerogen and increased clay crystallization and illitization (Reyes et al, 2022). Interestingly spring waters in the SHF center fall along curve 10 linking cwd (see Fig. 4B label) and a hypothetical water of serpentinization end-member (sph) similar in composition to the Marianas Trench water of serpentinization (sm) albeit with less seawater.

A plot of Cl vs $\delta^{18}O$ (Fig. 5A) shows discharges from Kapuni, Urenui, "McKee" wells, and Wharehuia along Line 1 linking a hypothetical high-Cl formation water and aqueous fluid with near-zero Cl and positive $\delta^{18}O$ akin to partial water of clay dehydration. The hypothetical formation water has a Cl composition near that of Kapuni-8 (32,000 mg/kg Cl). Water of clay dehydration (cw), with an average composition of $\delta^{18}O$= +19‰ and δD= -37‰ (Reyes et al, 2022) is expelled when smectite transforms to illitic clays during diagenesis at >100ºC (e.g., Völker and Stipp, 2015). Line 2 (Fig. 5A) indicates influx of meteoric water at Ngatoro, Kaimiro and a Kapuni well (Kapuni-11) and Maui, partly supported by results in Fig. 4A. The "McKee" well discharges (Mc), in a plot of Cl vs δD (Fig. 5B) fall along a mixing line (Line 1) of formation water with partial clay water of dehydration. Discharges with δD values above Line 1 (Fig. 5B) may be due to relatively recent input of seawater at Ngatoro and mixing of different formation waters at McKee (McKee-2 and 5A), Kapuni (Kapuni-11) and Waihapa wells. In contrast, well discharges from New Plymouth (P), Urenui and two Kapuni wells (Kapuni-KD1 and 8) have lower δD values than Line 1 and may be a result of decarboxylation of acetic or formic acid generated from vitrinites to produce CO_2, a process suggested by Killops et al (1996) for Taranaki.

In the SHF, variations in of $\delta^{18}O$ and δD with Cl (Figs. 5C and D) are attributed to mixing of porewater (pw) in the sedimentary formation (Cl= 10,000 mg/kg, δD= -14.1‰; $\delta^{18}O$= +7.2‰) with meteoric water (mw, Line 3), partial clay water of dehydration (Line 4) or clay water of dehydration (cw, Line 5). Fluids with $\delta^{18}O$ >+7.2‰ and Cl >10,000 (up to 25720 mg/kg) are due to contributions from waters of serpentinization generated just below the subduction interface. Solute concentrations (except for F) and δD in Na-Ca-

Cl are higher than in Na-Cl waters due to contributions and the effects of water of serpentinization. In contrast Na-Cl waters have higher $\delta^{18}O$ values and greater contributions from water of clay dehydration. In both fluids, seawater is a major component (Reyes et al, 2022).

In summary aqueous fluids discharged by Taranaki wells are a mixture of seawater, meteoric water, low-Cl water from clay dehydration, fluids generated from the maturation and oxidation of hydrocarbons, solutes from sedimentary rock and high-Cl formation waters from different sedimentary rock intervals at depth. The SHF has a similar set of fluid sources except for the strong presence of water of serpentinization ascending from the subduction interface.

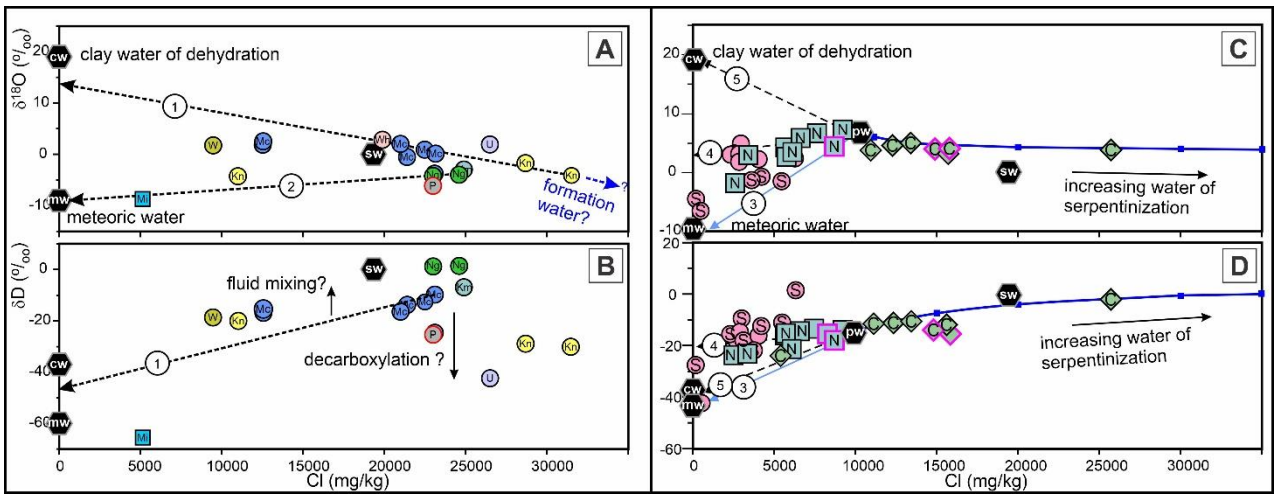

Figure 5: Aqueous fluid discharge [A] Cl vs $\delta^{18}O$ and [B] Cl vs δD in Taranaki and [C] Cl vs $\delta^{18}O$ and [D] Cl vs δD in the SHF (refer to Fig. 8 for symbols and Figs. 1, 11A and B for map locations of areas).

4.1.2 Temperatures

In most geothermal systems, whether high- or low-enthalpy, the Na-K and K-Mg geothermometers (Giggenbach, 1988) appear to be most reliable in predicting subsurface temperatures, where aqueous fluids interact with rock formations containing calc-alkaline components such as feldspars and micas. However, in low-enthalpy and hydrocarbon systems, water samples are best plotted on both the ternary Na-K-Mg and $10c_K/(10c_K+c_{Na})$ vs $10c_{Mg}/(10c_{Mg} + c_{Ca})$ to countercheck the veracity of near equilibrium conditions and Na-K temperatures (Reyes et al, 2010; 2022). Although most of the well discharge samples in Taranaki plot on the full equilibrium curve and within the partially equilibrated region of the Na-K-Mg ternary diagram, plots on the $10c_K/(10c_K+c_{Na})$ vs $10c_{Mg}/(10c_{Mg} + c_{Ca})$ diagram (Fig. 6A) reveal that most of the samples are far from equilibrium due to (1) the presence of drilling fluids, meteoric water and seawater that mask formation water compositions and (2) incomplete interaction of the rock with formation fluids. Thus, the use of the Na-K and K-Mg geothermometers in predicting subsurface temperatures in the Taranaki system may not necessarily give reliable results.

In contrast, the plots of SHF spring waters on the Na-K-Mg ternary diagram and $10c_K/(10c_K+c_{Na})$ vs $10c_{Mg}/(10c_{Mg} + c_{Ca})$ diagram (Fig. 6B) are in agreement with most points plotting on or near the full equilibrium curve or partially equilibrated region albeit with several samples affected by the influx of meteoric water and seawater. Overall, the Na-K temperatures at depth in the SHF is 90° ± 35°C with average values of 90°C in the south and north, and 100°C in the center.

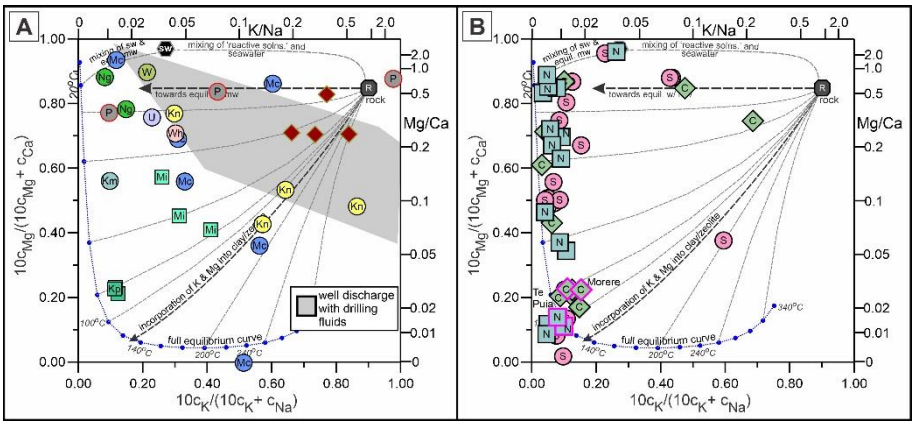

Figure 6: $10c_K/(10c_K+c_{Na})$ vs $10c_{Mg}/(10c_{Mg} + c_{Ca})$ plot of [A] Taranaki and [B] SHF aqueous fluid discharges (refer to Fig. 8 for symbols and Figs. 1, 11A and B for map locations of areas).

4.2 Gas

4.2.1 Sources

The isotopic $\delta^{13}C$ and δD compositions of CH_4 gas in both onshore and offshore Taranaki well discharges and spring discharges in the SHF mostly cluster within the region of oil-associated thermogenic gas, with one Maui well discharge extending to late-mature thermogenic (LMT) gas. Gases from Kaimiro (Km) in Taranaki and several springs from the south, center and north of the SHF are a mixture of thermogenic gas and CH_4 from secondary microbial (SM) methanogenesis (Fig. 7A).

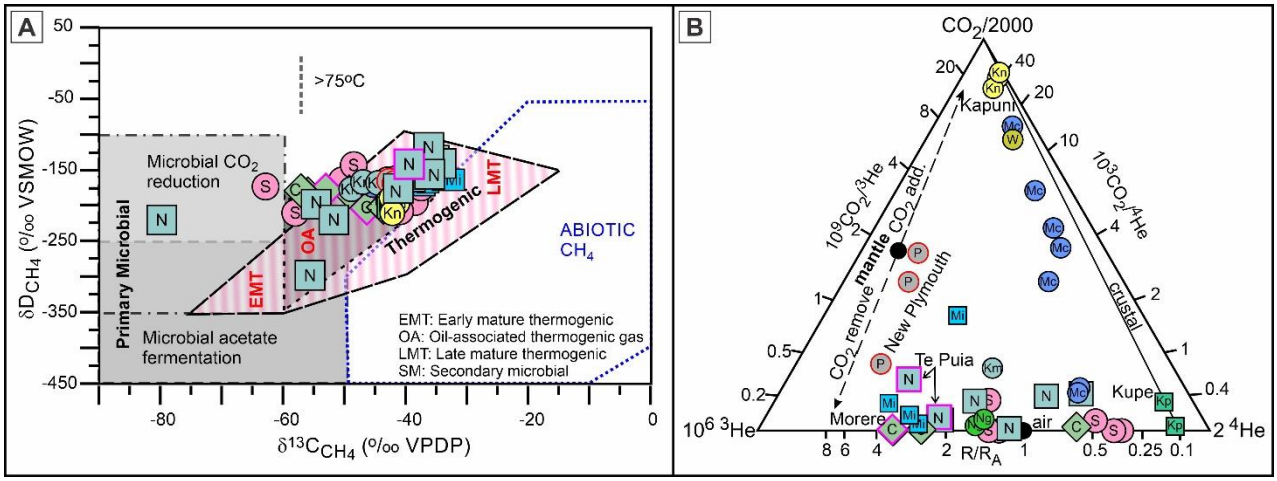

Figure 7: [A] $\delta^{13}C(CH_4)$ vs δD (CH_4) values for Taranaki and the SHF gas discharges after Milkov and Etiope (2018) and [B] relative contents of CO_2, ^3He and ^4He in Taranaki and SHF gas samples after Giggenbach et al (1993). R/R_A: ratio of mantle (^3He) to crustal helium (^4He) in the sample relative to R_A, the ratio in air (1.4×10^{-6}, Ozima and Podosek, 2002).

The ternary CO_2-^3He-^4He diagram in Fig. 7B shows that New Plymouth (P) and offshore Maui (Mi) well discharges in Taranaki plot nearest the mantle gas composition. In contrast, gases from Kapuni and offshore Kupe are largely crustal (Giggenbach, 1997). CO_2 gas is depleted in two of the New Plymouth wells and in offshore Maui whereas CO_2 is added during diagenesis at Kapuni (Kn), Waihapa (W) and some wells in the "McKee" (Mc) region. Despite proximity to the 1.8 Ma andesitic volcanic remnants, the relative concentrations of N_2, Ar, and ^4He in New Plymouth discharges (Reyes, 2021) show a high mantle component but no andesitic gas signature.

Samples from the SHF all plot at low relative CO_2 contents. The center and north of the SHF have the highest R/R_A with values of 3.35 (42% mantle gas component) in a cold well Gisborne-1 and 3.33 (42% mantle) in the Morere hot spring in the center, and 1.83-1.89 (23-24% mantle) in the north at Te Puia hot spring and Waimata cold spring in the north (Giggenbach et al, 1995; Reyes et al, 2022). Several cold spring discharges in the south and north are crustal (Fig. 7B). The high mantle component in the gases of the SHF appears to be related to the interconnectivity and depth of structures (down to the upper mantle) and the frequency of earthquakes: the deeper the structures and the more frequent the earthquakes during the time of sampling, the higher the mantle component in gas discharges (Reyes et al, 2022).

4.2.2 Temperatures and heat sources

A plot of relative CO_2, CH_4 and N_2 (Fig. 8A) corrected for air shows that discharges from the New Plymouth (P) and Kapuni (Ku wells have the highest relative CO_2 contents with median CO_2/CH_4 ratios of 2.0 and 1.0, respectively and CH_4-CO_2 temperatures >170ºC. Most of the wells in the "Mckee" region, Urenui, Te Kiri, Kaimiro and offshore Kupe are CH_4-rich with median CO_2/CH_4 ratios <0.05 and CH_4-CO_2 temperatures <125ºC. Stratford, Waihapa and offshore Maui well discharges are in between with median CO_2/CH_4 ratios of 0.15-0.42 and CH_4-CO_2 temperatures 140-155ºC. Although New Plymouth and Kapuni discharges have the highest gas temperatures, the sources of heat are different. The high mantle signature implies a shallowing of the hot upper mantle at New Plymouth. In contrast, the Kapuni gases are crustal in origin suggesting that advection of high temperature aqueous and gaseous fluids may be rapidly circulated along deep crustal structures.

The CO_2/CH_4 ratios of gas samples in the SHF are mostly much lower than in Taranaki, ranging from 0.0003 to 0.105 (Fig. 8B) with the average ratios increasing from south to north: 0.0026 in the south (range: 0.0003-0.95), 0.0031 in the center (range: 0.0004-0.08) and 0.0087 in the north (range: 0.002-0.105). The CO_2/CH_4 ratios increase with increasing average CH_4-CO_2 temperatures from 80ºC in the south, 85ºC in the center, to 100ºC in the north consistent with hotter crust and higher heat flow in the north (Field et al, 1997) and in part, deeper fluid sources in the north where more structures are interconnected with other structures down to the subduction interface at >10 km where temperatures are 185º $\pm$ 25ºC; and even extending to the upper mantle (Reyes et al, 2022).

5. DISCUSSION

5.1 Trends

The positive correlation between R/R_A values with estimated heat flow values in Taranaki suggest that the depth of the hot upper mantle is shallowest at New Plymouth (heat flow values: 70-74 mW/m^2) and deepest in offshore Kupe (heat flow value: 50 mW/m^2; Figs. 2A and 9A). The highest median mantle component onshore, assuming a value of $8R/R_A$ for the mantle (Simmons et al, 1987), is at New Plymouth at ~60% and at Kaimiro and Ngatoro at ~25% with the lowest in the "McKee" region, Waihapa and Kapuni.

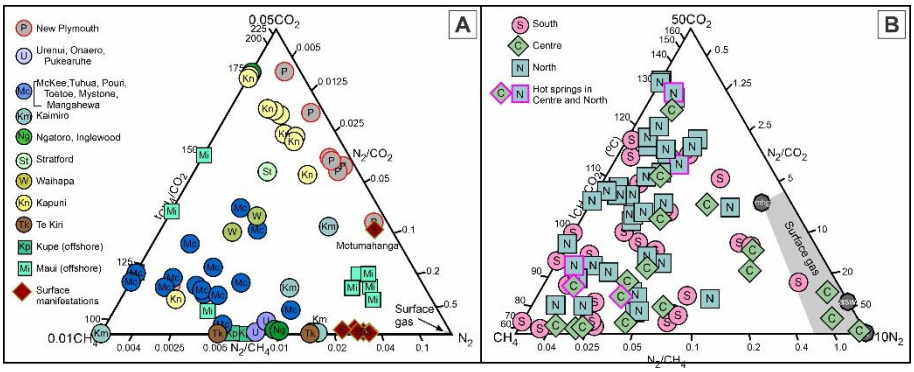

Figure 8: Ternary CO_2-N_2-CH_4 diagram showing CH_4-CO_2 temperatures on the left for discharges from [A] well and surface manifestations in Taranaki and [B] surface manifestations in the subaerial Hikurangi forearc, East Coast. Surface gas is mostly air (a), air-saturated water (asw) and marsh gas (mhg). Note the scale difference between the two graphs.

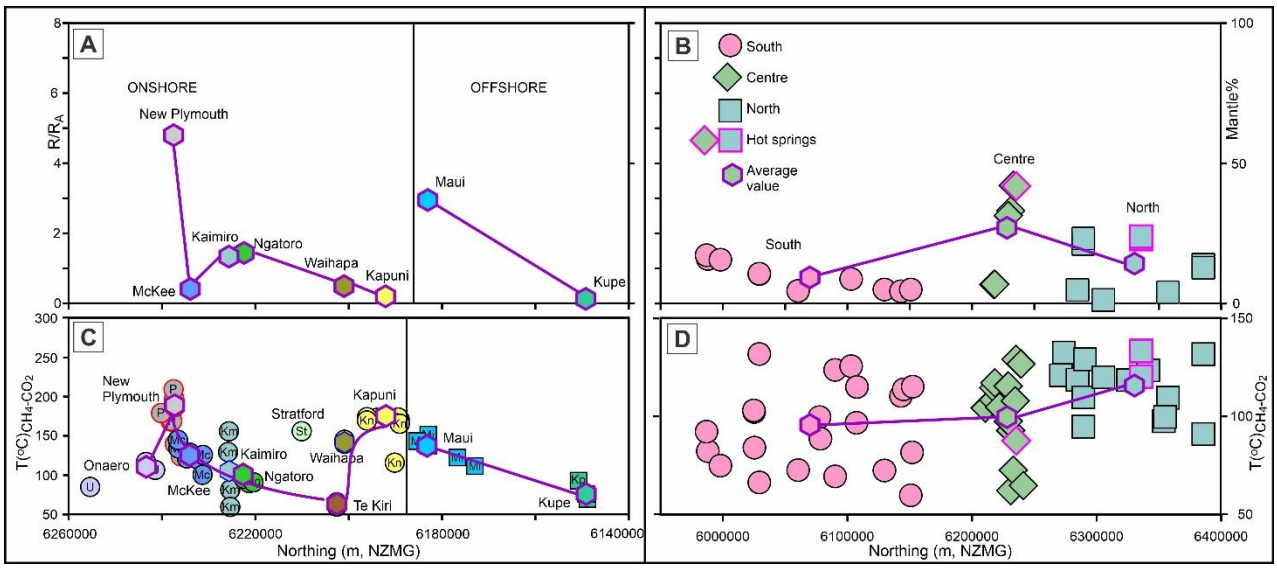

Figure 9: North-south trend of R/R_A values and mantle% in [A] various Taranaki areas (median values) and [B] SHF (individual and median values) and CH_4-CO_2 gas temperatures in [C] Taranaki and [D] SHF (refer to Fig. 8 for symbols). Note that gas temperature scales are different between Taranaki and the SHF.

However, as shown in Fig. 9C, high mantle input does not necessarily correlate with high subsurface temperatures. Although New Plymouth discharges have the highest mantle signature and the highest CH_4-CO_2 gas temperatures (>200ºC), discharges from Kapuni and "Mckee", with crustal or near-crustal signatures (near 0% mantle input), have temperatures (125-175ºC) higher than Kaimiro and Ngatoro (<125ºC) where mantle input is ~25%. It is possible that advection of high temperature fluids in regions of low heat flow and low mantle input may be caused by deep permeable structures that act as channels for the rapid ascent of hot fluids, similar to springs in the SHF (Figs. 9B and D; Reyes et al, 2010 and 2022).

To determine probable depths of thermal reservoirs in Taranaki and the SHF, the BHT (bottomhole temperature) of abandoned wells and estimated CH_4-CO_2 temperatures of gases discharged by wells and surface manifestations are plotted along north-south transects for Taranaki (Fig. 10A) and the SHF (Fig. 10B). The general source depth of high-temperature gases, in the plots, assumes a steady state conductive regime, which is untrue because of evidence for fluid advection in both areas. Nevertheless, Fig. 10A shows that thermal reservoirs in Taranaki with temperatures >100ºC have been intersected by wells drilled at Kapuni, Waihapa, Stratford-Wharehuia, Ngatoro, Kaimiro, the McKee region and New Plymouth. Deepening wells in Kapuni and New Plymouth may increase the chances of intersecting 170-180ºC and 200ºC advecting fluids, respectively. The highest temperature of the thermal reservoir in the SHF is 140ºC, within the Rotokautuku heat flow anomaly (Fig. 2B). None of the wells in the south (Fig. 10B) and only one well each in the center and north of the SHF intersected the hot thermal reservoir. Hence, if any geothermal retrofitting is planned for the SHF, wells should be drilled down to at least 3-3.5 km in most of the SHF and at least 2.5 km at Rotokautuku.

Figure 11A is a map showing general deep temperatures in the different regions of Taranaki. The highest temperatures at >150ºC occur at New Plymouth, Kapuni and possibly Stratford, with 100-150ºC at Urenui, the "McKee" region, Ngatoro, Kaimiro and Waihapa and <100ºC at Te Kiri and offshore Kupe. The thermal reservoirs >100ºC in Taranaki can be intersected by wells drilled to 3.0 to >4.5 km, depending on the area. Several wells in Taranaki have already intersected >100ºC thermal reservoirs. Figure 11B shows the depth at which the 100ºC thermal reservoir may be intersected in the SHF: ~3.5 km in the upper south and center and ~3.0 km in the north except for Rotokautuku at ~2.5 km.

Unlike geothermal systems in volcanic regions of New Zealand (Taupo Volcanic Zone and Ngawha) and low-enthalpy hot spring systems outside the main geothermal power-producing areas, gases in Taranaki and the SHF contain a high percentage of >C6 that may condense in the separator and pipelines as pressures and temperatures change (Figs. 12A and B). In Fig. 12A, the cricondenbar is the maximum pressure above which no gas can be formed regardless of the temperature and the cricodentherm the maximum temperature above which liquid cannot be formed regardless of pressure (Dustman et al, 2006). Figure 12B shows that for a given pressure, liquid hydrocarbons with varying C_n will condense at different temperatures. If hot fluids from petroleum wells will be directly harnessed for geothermal heat or power then the construction of phase diagrams from the hydrocarbon chemical composition, similar to Figs.12A and B, are essential in predicting the behavior of hydrocarbon phases during well production (e.g., Wang and Economides, 2010), for example, by setting conditions to minimize condensation of hydrocarbon gases either by controlling the temperature and or the pressure (e.g., choking) in the separator and distribution lines. However, as suggested previously (Reyes, 2019) the heat from abandoned petroleum wells for direct heat and power production can simply be harnessed using closed-loop deep borehole heat exchangers (e.g., Zhu et al, 2019).

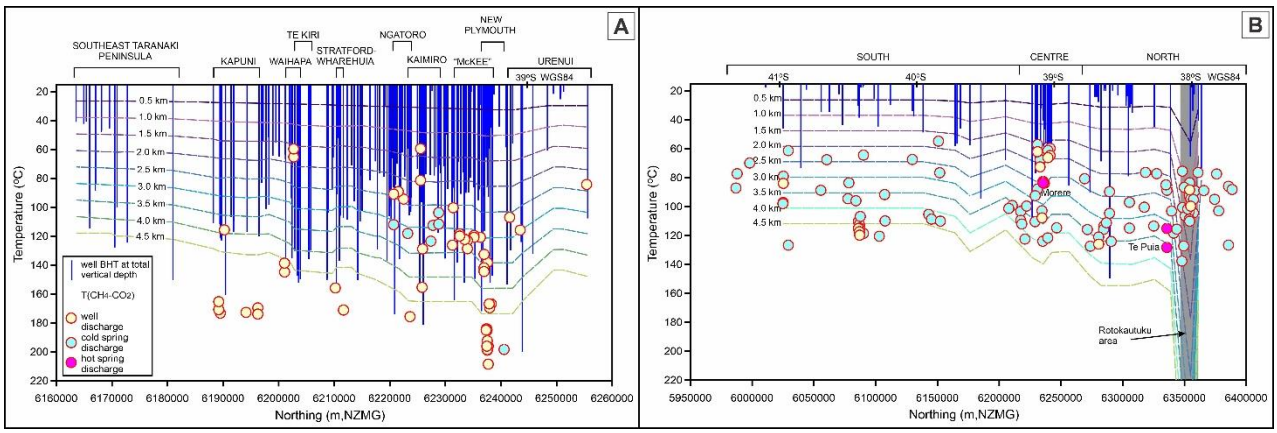

Figure 10: North-south distribution of well bottomhole temperatures (BHT), depth contours, and CH_4-CO_2 temperatures of well and natural surface discharges in [A] Taranaki and [B] SHF.

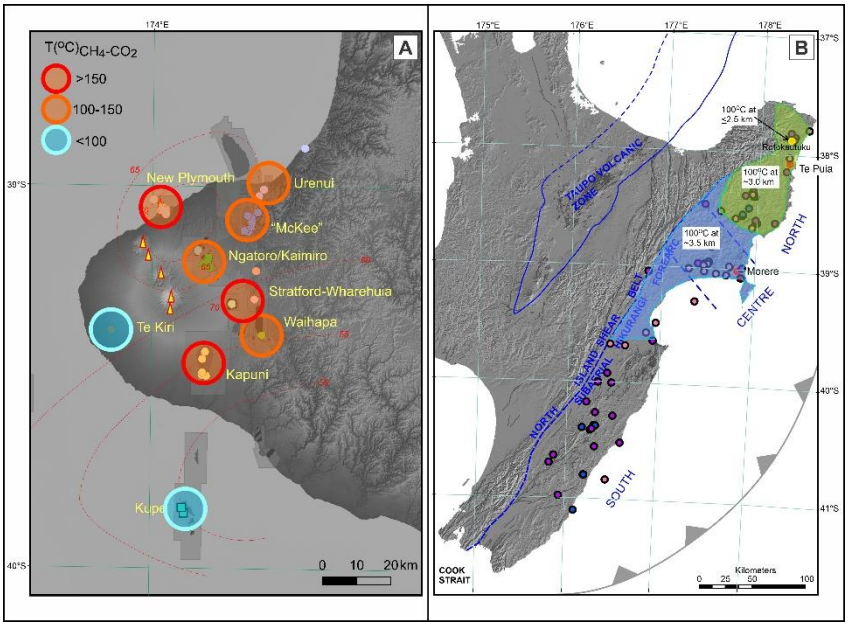

Figure 11: Map showing viable areas for possible geothermal exploration and exploitation in [A] Taranaki where discharge fluid temperature ranges are indicated and [B] SHF where the general depth of the 100ºC isotherm can be intersected by a well.

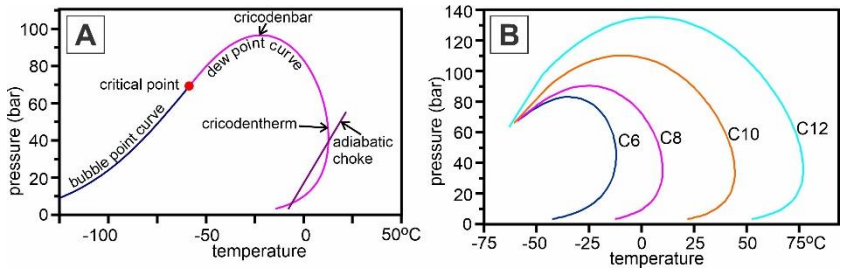

Figure 12: Simplified phase diagrams for a volatile hydrocarbon system showing temperature vs pressure [A] from the bubble to the dew point curves. Only liquid exists above the bubble point curve and only vapor beyond the dew point curve. Two-phase fluids occur between the bubble and dew point curves; [B] dew point curves for alkane gases C_6 to C_{12} (from Dustman et al, 2006).

6. CONCLUSION

Subsurface temperatures at Taranaki and the northern part of the SHF show that geothermal energy can be harnessed for power generation and direct heat use. The highest subsurface temperatures based on solute chemistry occur at New Plymouth, Kapuni and Stratford (>150ºC), with moderate temperatures (100-150ºC) at Onaero, Kaimiro, Ngatoro, McKee and Waihapa. The lowest temperatures occur in the west at Te Kiri (<100ºC). High temperatures at New Plymouth may be related to the shallowing of the upper mantle in this Taranaki region but high temperatures at Kapuni and Stratford may be related to rapid hot fluid ascent through deep faults, similar to the northern region of the SHF.

REFERENCES

Allis, R.G., Funnell, R.H. and Zhan, X.: From basins to mountains and back again: NZ basin evolution since 10 Ma. *Proceedings* of the 9th International Symposium on Water-Rock Interaction, Taupo, New Zealand, (1998), 3-9.

Cook, R.A., Sutherland, R., Zhu, H. and others (1999): Cretaceous-Cenozoic geology and petroleum systems of the Great South Basin, New Zealand, Institute of Geological and Nuclear Sciences Monograph, 20, (1999), 188p.

de Courcy Clarke, E.: The geology of the New Plymouth subdivision, Taranaki division. New Zealand Geological Survey Bulletin 14, Wellington. (1912)

Dustman, T., Drenker, J. Bergman, D.F., Bullin, J.A.: An analysis and prediction of hydrocarbon dew points and liquids in gas transmission lines. Questar Pipeline Company report, 18p. (2006)

Ellis, A.J., and Mahon, W.A.J.: Natural hydrothermal systems and experimental hot water/rock interactions (Part II). *Geochimica et Cosmochimica Acta*, **31**, (1967), 519-538.

Field, B.D., Uruski, C.I and others: Cretaceous-Cenozoic geology and petroleum systems of the East Coast region, New Zealand, Institute of Geological and Nuclear Sciences Monograph, 19, New Zealand, (1997), 301p.

Funnell, R. and Allis, R.G.: Hydrocarbon maturation potential of offshore Canterbury and Great South basins, *Proceedings* 1996 New Zealand Petroleum Conference, New Zealand, (1997), 22-30.

Funnell, R., Chapman, D., Allis, R., Armstrong, P.: Thermal state of the Taranaki Basin, New Zealand, *Journal of Geophysical Research*, **101(B11)**, (1996), 25,197-25,215.

Giggenbach, W.F.: Geothermal solute equilibria. Derivation of Na-K-Mg-Ca geoindicators. *Geochimica et Cosmochimica Acta*, **52**, (1988), 2749-2765.

Giggenbach, W.F., Sano, Y., Wakita, H.: Isotopic composition of helium, and CO2 and CH4 contents in gases produced along the New Zealand part of a convergent plate boundary. *Geochimica et Cosmochimica Acta*, **57**, (1993), 3427-3455.

Giggenbach, W.F., Stewart, M.K., Sano, Y., Goguel, R.L. and Lyon, G.L.: Isotopic and chemical composition of solutions and gases from the East Coast accretionary prism, New Zealand. *IAEA-TECDOC*, **788**, (1995), 209–231.

Henderson, J., and Ongley, M.: The geology of the Mokau subdivision. New Zealand Geological Survey Bulletin 24, Wellington (1923).

Killops, S.D., Allis, R.G., Funnell, R.H.: Carbon dioxide generation from coals in Taranaki Basin, New Zealand: implications for petroleum migration in Southeast Asian Tertiary basins. *AAPG Bulletin*, **80(4)**, (1996), 545-569.

King, P.R., Thrasher, G.P.: Cretaceous-Cenozoic geology and petroleum systems of the Taranaki Basin, New Zealand, Institute of Geological and Nuclear Sciences Monograph 13, (1996), 243 p.

Liu, X., Falcone, G. and Alimonti, C.: A systematic study of harnessing low-temperature geothermal energy from oil and gas reservoirs. *Energy*, **142**, (2018), 346-355.

Locke, C.A., Cassidy, J., MacDonald, A.: Constraints on the evolution of the Taranaki volcanoes, New Zealand, based on aeromagnetic data. *Bulletin of Volcanology*, **56**, (1994), 552-560.

Lyon, G.L., Giggenbach, W.F. and Sano, Y.: Variations in the chemical and isotopic composition of Taranaki gases and their possible causes. *Proceedings* New Zealand Petroleum Conference, (1996).

Milkov, A.V. and Etiope, G.: Revised genetic diagram for natural gases based on a global dataset of >20,000 samples. O*rganic Geochemistry*, **125**, (2018), 109-120.

Ozima, M., Podosek, F.A.: Noble gas geochemistry. Cambridge University Press, UK, (2002), 302p.

Palmer, J.A. and Andrews, P.B.: Cretaceous-Tertiary sedimentation and implied tectonic controls on the structural evolution of Taranaki Basin, New Zealand. In: Balance, P.B. (Ed.) South Pacific sedimentary basins. Sedimentary basins of the world, Elsevier, Amsterdam, (1993), 309-327.

Reyes A.G., Christenson, B.W., Faure, K.: Sources of solutes and heat in low-enthalpy mineral waters and their relation to tectonic setting, New Zealand. *Journal of Volcanology and Geothermal Research*, **192**, (2010), 117-141.

Reyes, A.G. and Hall, D.L.: Te Puia Springs, Gisborne, past and present fluids, *Proceedings* 44th New Zealand Geothermal Workshop, Auckland, New Zealand (2022).

Reyes, A.G., Ellis, S.M., Christenson, B.W. and Henrys, S.A.: Fluid flowrates and compositions and water-rock interaction in the Hikurangi margin forearc, New Zealand. *Chemical Geology*, **614**, (2022), doi: 10.1016/j.chemgeo.2022.121169

Reyes, A.G.: Abandoned oil and gas wells: a reconnaissance study of an unconventional geothermal resource. GNS Science report 2007/23, Lower Hutt, New Zealand, (2007) 36 p.

Reyes, A.G.: Geochemistry and geothermal prospectivity of the hydrocarbon-producing Taranaki sedimentary basin. *Proceedings* 43rd New Zealand Geothermal Workshop, Auckland, New Zealand, (2021).

Reyes, A.G.: Geothermal energy from abandoned petroleum wells in New Zealand. *Proceedings* 12th Asian Geothermal Symposium, Daejeon, Korea, (2018).

Reyes, A.G.: Geothermal energy from petroleum wells in New Zealand: benefits and hurdle. *Proceedings* 41st New Zealand Geothermal Workshop, Auckland, New Zealand, (2019).

Reyes, A.G.: Hydrothermal and diagenetic history of the Mangahewa Formation in Mangahewa-2 well, Taranaki, Ministry of Economic Development Petroleum Report 2894, Wellington, New Zealand, (1998), 113p.

Reyes, A.G.: Low-temperature geothermal reserves in New Zealand. *Geothermics*, **56**, (2015), 138-161.

Simmons, S.F., Sawkins, F.J., Schlutter, D.J.: Mantle-derived helium in two Peruvian hydrothermal ore deposits. *Nature*, **329**, (1987), 429-432.

Smale, D., Mauk, J.L., Palmer, J., Soong, C.W.R., Blattner, P.: Variations in sandstone diagenesis with depth, time, and space, onshore Taranaki wells, New Zealand. New Zealand. *Journal of Geology and Geophysics*, **42(2)**, (1999), 137-154.

Townend, J., Sherburn, S., Arnold, R, Boese, C. and Woods, L.: Three-dimensional variations in present-day tectonic stress along the Australia–Pacific plate boundary in New Zealand. *Earth and Planetary Science Letters*, **353-354**, (2012), 47-59.

Townsend, D.B., Vonk, A., Kamp, P.J.J. (comps): Geology of the Taranaki area: scale 1:250,000. Institute of Geological & Nuclear Sciences 1:250,000 geological map 7, 77 p. + 1 folded map (2008)

Völker, D. and Stipp, M.: Water input and water release from the subducting Nazca Plate along southern Central Chile (33oS–46oS). *Geochem. Geophys. Geosyst.*, **16**, (2015), 1825-1847.

Wang, X., Economides, M.: Advanced natural gas engineering. Gulf Publishing Company, 368p. (2010)

Wang S., Yan, J., Hu, J., and Li, K.: Exploitation and utilization of oilfield geothermal resources in China. *Energies*, **9**, (2016), doi:10.3390/en9100798.

Wanner, C., Eichinger, F., Jahrfeld, T. and Diamond, L.W.: Causes of abundant calcite scaling in geothermal wells in the Bavarian Molasse Basin, Southern Germany. *Geothermics*, **70**, (2017), 324-338.

Williams, C.A., Eberhart-Phillips, D., Bannister, S., Barker, D.H.N., Henrys, S.A., Reyners, M.E., Sutherland, R. Revised interface geometry for the Hikurangi subduction zone, New Zealand. *Seismological Research Letters*, **84(6)**, (2013), 1066-1073.

Zhu, Y., Li, K., Liu, C., and Mgijmi, M.B.: Geothermal power production from abandoned oil reservoir using in situ combustion technology. *Energies*, **12**, (2019), doi: 10.3390/en12234476.